Numerical Investigation of Solar Energy Driven Diffusion Absorption Refrigeration Cycle

Kishan Pal Singh*‡, Onkar Singh**

*Department of Mechanical Engineering, Ph.D. Scholar, A.K.T.U, Lucknow, (U.P.) - India

** Department of Mechanical Engineering, Faculty of Engineering, H.B.T.U, Kanpur, (U.P.) - India

(kishan_amu@rediffmail.com, onkpar@rediffmail.comecond)

‡ Corresponding Author email id;,kishan_amu@rediffmail.com

Received: 04.06.2018 Accepted:07.08.2018

Abstract- The refrigeration requirements are stringent in the countries which have ample sunshine and the technological solutions based upon solar radiations for meeting the refrigeration requirements could a boon. The present work deals with the development of a diffusion absorption cycle based refrigeration system operated by solar energy. This study focuses on the thermodynamic modelling of NH_3 - H_2O diffusion absorption refrigeration cycle with helium as pressure equalizing gas. Results obtained from the parametric analysis shows that 1.3% profit in refrigerating effect is observed when 3 °C sub-cooling occurs in condenser. The coefficient of performance gain gets up to 24% for ammonia mass fraction ranges from 0.28 to 0.58 as compared to the DAR cycle using saturated condensed liquid. A loss of 3.02% in coefficient of performance is seen for 10°C decrease in evaporator temperature. A range of the generator temperature lies between $140°C \leq T_g \geq 160°C$ is best suited for optimum coefficient of performance.

Keywords Diffusion, pressure equalizing gas, aqua ammonia solution, absorption, coefficient of performance and atmospheric temperature.

1. Introduction

The first diffusion absorption system was based on three fluid system invented by Von Platen and Munters in the year 1922 and got patent in 1923 [1, 2]. In this cycle, aqua ammonia used as working fluids and hydrogen as pressure equalizing inert gas. Zohar *et al.* [3] developed a model for DAR cycle manufactured by Dometic Sweden to investigate the cycle performance. They were getting maximum value of coefficient of performance at the ammonia concentrations in rich solution lies in between 0.25 to 0.30 and in lean solutions is 0.10, for the generator temperature lies between 195 °C to 205 °C. Numerical analysis carried out by Giuseppe Starace et al. [4] shows when the desorber temperature increases beyond 150°C, the rich solution mass flow rate drops off to the refrigerant. Hence, cooling capacity lessens, consequently coefficients of performance decreases. The results showed the difference of 6.1%, 8.5%, and 2% in rich, poor and coefficient of performance respectively.

Srikhirin et al [5] tested a heat power driven DAR system with heat input from 1000 W to 2500 W using aqua ammonia as working fluid and helium as pressure equalizing gas at vapour pressure 6.1 bar. The system cooling found to be between 100 W to 180 W having coefficient of performance between 0.09 and 0.16. The impact of mass transfer abilities by the evaporator and absorber has a great effect of on the system performance. Some researchers used different pairs of refrigerant and absorbent. Wang Q. et al [6] worked on a DAR system using amalgam refrigerant R23/ R134a, DMF as absorbent and helium as auxiliary gas. It was seen that for the best performance of the DAR system, the generating temperature should be in the range of 110-160 °C and the system total pressure should be in the range of 9 bar to 26 bar. Sözen et al. [7] analysed three DAR cycles having different configurations in which first DAR was similar to Electrolux refrigerator. In this configuration, condensate is sub cooled before evaporator entrance. In the next DAR, the saturated condensate was supplied to evaporator while in last DAR, an ejector placed at absorber inlet in the absorber. The study showed a 40% reduction in energy consumption for relatively low temperature (~ 6 °C) by DAR-3 for the same cooling area.

Ben Ezzine et al. [8, 9] numerically investigated DAR cycle with working fluid R124/DMAC and light hydrocarbon

mixture as working fluid and helium as inert gas. In the paper [8], simulation carried out for ambient temperature ranges from 27 °C to 35 °C and the driving generator temperature ranges from 90 °C to 180 °C. The result obtained shows that the capacity to attain lowest temperature in evaporator and performance of the system are largely dependent up on the absorber efficiency and the generator temperature. The fluid mixture [8] used for refrigeration showed a higher coefficient of performance at lower generator temperature as compared to aqua ammonia system. This pair of working fluid also works on lower vapour pressure for inert gas and provides to decrease wall thickness of system. Ben Ezzine et al. [9] studied using binary hydrocarbon mixture (C_4H_{10}/C_9H_{20}) as working fluid with helium as auxiliary gas. The results shows that for the range (120-150 °C) of generator temperature, at the generator temperature 138 °C, the lowest evaporator temperature attained was -10 °C.

Handong Wang [10] studied a DAR system with using $LiNo_3$-NH_3-He as working fluid and a spray absorber with plate type to optimize the mass and heat transfer. This study shows that evaporator temperature mainly depends upon absorber temperature rather than generator and condenser temperature. It shows the lowest evaporator temperature is of -13 ºC, corresponding refrigerating capacity and coefficient of performance are 1.9 kW and 0.156 at heat source, generator, absorber and condenser temperature 92.7 ºC, 87 ºC, 29.6 ºC and 21.6 ºC, respectively. Chen et al [11] analysed newly designed generator with heat exchanger to reuse waste heat from the rectifier to heat the weak absorbent from the reservoir. The test results of the DAR with new designed generator were compared with baseline tests. The new generator design illustrated a 50% increase in COP with the same cooling capacity compared to baseline tests. In different studies [1-11], the effects of pressure losses in fluid flow in pipe due to friction and dynamic pressure losses in different components of the DAR system is assume negligible. Acuna A. et al. [12] presented in their study that the best option for transfer of heat between the hot fluids circulating in solar compound parabolic collector and the cooling refrigerants pair of DAR cycle is glycerol-water ($C_3H_8O_2$-H_2O). Koyfman et al. [13] investigated the performance of the bubble pump for diffusion absorption refrigeration experimentally. It can be seen that the bubble pump operates at slug flow regime with a churn flow regime at the entrance of the bubble pump tube. Zohar et al [14] studied influence of the generator and bubble pump configuration on the performance of DAR cycle. Ahmed Q.K. [15] studied numerically for a developed design of a solar collector using fluent software. This study shows value of mean storage temperature was 18 °C in a particular day of winter season and 41 °C in summer season. It was also observed that the mean storage temperature of the water inside the collector decrease with increasing the volume of the collector.

In this work, detailed thermodynamic models for three generator and bubble pump configurations were developed: (a) heat input into the rich solution with no heat transfer to the poor solution; (b) heat input into the rich solution with heat transfer to the poor solution in the annular; and (c) heat input into the rich solution through the poor solution, thus also desorbing refrigerant from the poor solution, with heat transfer to the poor solution. The performance of three DAR systems, which differ in their generator and bubble pump configuration, was studied numerically.

It is evident from the published work that the effects of pressure losses have significant impact and could deviate, the experimental results from the theoretical results. In the present study, a basic DAR cycle operating with ammonia as refrigerant and water as absorbent with helium as pressure equalizing gas is investigate, taking into account pressure losses and having all process are the same except condensate liquid flows to the evaporator considering as sub-cooled liquid. The study shows that at lower generator temperature piping and dynamic pressure affects the coefficient of performance while at higher generator temperature pressure effects can be neglected.

In view of Indian climatic conditions where the ambient temperature raises up to 44 °C in summer season and falls down up to 8 °C in winter season. Therefore, the operating range of the DAR cycle should match with the availability of solar radiation to run the system round the year.

2. Model Description

Figure 1 shows the schematic diagram of solar energy operated DAR cycle. The DAR model constitutes an evaporator, a condenser, a rectifier, a solution heat exchanger, a flash box, an absorber, a receiver tank and a generator. The generator is a combination of bubble pump and boiler. The bubble pump is a cylindrical concentric hollow tube used to raise fluid from lower level to higher level due to thermosyphon effect. The DAR cycle operated mainly in three circuits. These three circuits are solution circuits, refrigerants circuits and gas circuits. Two circuits of DAR cycle are similar to the conventional absorption cycle except its third gas circuits. This circuit helps to circulate vapour between the absorber and the evaporator. The solution circuit includes the generator, bubble pump, absorber, and receiver tank and solution heat exchanger. The refrigerant circuit contains all components of DAR cycle because refrigerant ammonia passes through all components. The gas circuit contains evaporator, absorber, receiver tank and flash box. The pressure equalizing inert gas passes through the gas circuits.

The working of cycle starts from the absorber. The rich in ammonia solution comes from receiver tank at state 12 through the solution heat exchanger. This rich solution heats by transfer of heat from the hot counter flow lean solution in the SHX, which returns from the rectifier and separator through outer concentric pipe of bubble pump at state 13. The pre heated rich solution flows into the generator at state 1. This rich solution is further heat by the driving thermal power Q_g at state 2, provides form solar energy in this arrangement as shown in diagram. The rich solution starts boiling and form bubbles of ammonia vapour, which raises carrying slugs of lean solution through bubble pump to the separator state 4. Lean solution flows down from separator at state 3, through outer pipe of bubble pump. To remove any possibilities of liquid drops present in evaporated refrigerant

vapours, vapour passes through the rectifier. In the rectifier, solution droplets filter, rejecting heat Q_r and revert back to state 3 through state 5. Now the almost pure refrigerant vapours at state 6 enter into the condenser, which is a finned tube with natural convection cooling. In condenser, refrigerants vapour starts de-superheating and condenses into liquid at total system pressure after rejecting heat to the cooling medium of the condenser. The uncondensed refrigerant vapours, if any, by passes to the receiver tank through the state 8. The condensed refrigerant liquid at state 7 drifts into the flash box, where it mixes with inert gas adiabatically to reduce partial pressure of refrigerant liquid and enters into the evaporator at state 9. The pressure equalizing gas with minor content of ammonia gas residual leaving the absorber at state 11 and enters into the flash box. The partial pressure of liquid refrigerant reduces and allows evaporating at lower temperature. The evaporation of refrigerant extracts heat Q_e from the evaporator cabin providing refrigeration effect. From the evaporator, mixtures of refrigerant and pressure equalizing gas return to the receiver tank at state 10.

The ammonia and helium gas mixture enters into absorber coil from bottom and flows upward while lean solution enters into absorber coil from the top at state 14 and flows downward in a counter flow arrangement. Ammonia vapours are readily absorbed in the lean liquid solution rejecting heat Q_a to the cooling medium of the absorber, which consequently forms rich solution drifting to the receiver tank. Helium gas is not absorbed and continues to flow to the evaporator with ammonia residuals at state 11. The circulation circuit of helium and ammonia gas is driven by natural convection caused primarily by the larger density difference associated with the ammonia mass fraction in vapour. The rich solution leaves the receiver tank at state12 and flows towards the generator. Thus, the DAR cycle is complete.

One of advantages of DAR cycle is that it is a self-circulating cycle and the circulation occurs due to density and gravity differences of working fluid. The thermodynamic modelling of DAR system has been done to study and evaluate the thermodynamic performance of DAR cycle. The modelling details for various components of DAR cycle are as under.

3. Thermodynamic Modelling

For the ease of thermodynamic modelling, some assumptions and considerations as detailed ahead, are used in the present study.

- Solution heat exchanger effectiveness is constant.
- Mixing of refrigerant liquid and inert gas in flash box is adiabatic.
- The gas mixture behaves like an ideal gas. The property of mixture calculates according to the ideal gas considerations.
- The ambient temperature, generator and evaporator temperature are specified.
- Pressure loss in pipe flow and dynamic pressure losses in components are considered as specified in input parameters.
- The components and piping of DAR cycle are thermally insulated properly.
- There is no absorption-taking place in the receiver tank.
- Ammonia refrigerant after rectification is 99.5% pure.
- The cooling medium for condenser is air. Therefore, the condensation temperature will be ambient temperature. This assumption will provide a proper temperature gradient for heat transfer between refrigerant and condensing medium. The condensation medium for both condenser and absorber is same (i.e. $T_{12} = T_7$).
- The temperature of the refrigerant and of the pressure equalizing inert gas leaving the evaporator is same (i.e. $T_{10} = T_{10,1}$).
- There is no temperature difference between lean solution and vapour bubbles leaving the generator; i.e. both are at equal temperature ($T_3 = T_4$).

3.1 Governing equations used in thermal modelling of diffusion absorption refrigeration cycle

The thermodynamic analysis of vapour absorption cycle is based on the following three governing equations.

i. Mass balance $\sum m = 0$

ii. Material balance (or partial mass balance) $\sum m\xi = 0$

iii. Energy balance $\sum Q + \sum \dot{m}h = 0$

The mass, ammonia mass balance and energy balance equations for various components of the DAR cycle are present below.

3.2 Generator, bubble pump and separator as a unit

For simplification of balancing, combines generator, bubble pump and separator. The generator used to heat-up the rich in ammonia solution coming from state1. Vapours of ammonia with water are produce and slug flow induced in bubble pump with liquid portion of solution and rise to the separator and then flows to the rectifier after lean solution removal.

General mass balance equation

$$m_2 = m_3 + m_4 \quad (1)$$

Where $m_1 = m_2$

Ammonia mass balance equation

$$m_2\xi_2 = m_3\xi_3 + m_4\zeta_4 \quad (2)$$

Energy balance equation

$$\dot{Q}_g = \dot{m}_3h_3 + \dot{m}_4h_4 - \dot{m}_2h_2 \quad (3)$$

3.3 Rectifier

The rectifier has the gaseous ammonia-water solution at state 4 being cooled to produce almost pure vapour ammonia refrigerant at state 6 and condensed lean in ammonia solution returns at state 5 into the separator to form lean solution at

state 3. Thus, energy balance equation for rectifier gives the heat rejection from the rectifier as:

General mass balance equation

$$\dot{m}_4 = \dot{m}_5 + \dot{m}_6 \quad (4)$$

Ammonia mass balance equation

$$\dot{m}_4\zeta_4 = \dot{m}_6\zeta_6 + \dot{m}_5\xi_5 \quad (5)$$

Or $\dot{m}_6 = \frac{\zeta_4 - \xi_5}{\zeta_6 - \zeta_4}\,\dot{m}_5$ (6)

Energy balance equation

$$\dot{Q}_r = \dot{m}_5 h_5 + \dot{m}_6 h_6 - \dot{m}_4 h_4 \quad (7)$$

3.4 Condenser

Pure ammonia vapour after leaving the rectifier at state 6 condenses by transferring heat to the ambient air at constant pressure.

General mass balance equation

$$\dot{m}_7 = \dot{m}_6 \quad (8)$$

Ammonia mass balance equation

$$\zeta_7 = \zeta_6 \quad (9)$$

Thus heat rejected to cooling medium in the condenser can be written as

$$\dot{Q}_c = [\dot{m}_7 X_7 h_{7f} + \dot{m}_8 X_8 h_{8v} - \dot{m}_6 h_6] \quad (10)$$

Where, $X_7 = (1 - X_8)$

The liquid fraction of the refrigerant at state 7 comes from the condenser, while the vapour fraction of the refrigerant, if any, by passes to the receiver tank.

3.5 Flash Box

Liquid ammonia at state 7 mixes with helium gas with some residual ammonia gas at state 11 in the flash box. This causes pressure of both ammonia and helium to drop and mixtures of ammonia and helium gas with their respective partial pressures enters the evaporator at state 9. Mass balance and energy balance for flash box chamber are present below.

Mass flow rate of ammonia vapour after expansion

$$\dot{m}_{9g} = [\dot{m}_7 + \dot{m}_v]\, X_9 \quad (11)$$

X_9 is the dryness fraction of ammonia vapour after adiabatic mixing and expansion at state 9.

Mass flow rate of ammonia liquid after expansion in flash box

$$\dot{m}_{9l} = [\dot{m}_7 + \dot{m}_v]\,(1 - X_9) \quad (12)$$

General mass balance of ammonia at exit of flash box at state 9

$$\dot{m}_{9l} + \dot{m}_{9g} = \dot{m}_{R9} \quad (13)$$

$$\dot{m}_{9l} + \dot{m}_{9g} = \dot{m}_7 + \dot{m}_v \quad (14)$$

Energy balance equation for sub cooled ammonia refrigerant, helium and ammonia residual gas leaves at expansion at state 12

$$\dot{m}_v h_{11} + \dot{m}_H h_{H,11} + \dot{m}_7 h_7 = \dot{m}_H h_{H,9} + \dot{m}_{9l} h_{9l} + \dot{m}_{9g} h_{9g} \quad (15)$$

3.6 Evaporator

Liquid ammonia at state 9 enters into the evaporator. For ease of balancing equation, the following mass flow rate are defining as

Mass flow rate of ammonia vapour after expansion

$$\dot{m}_{9v} = [\dot{m}_7 X_7 + \dot{m}_{ar}] X_9 \quad (16)$$

Mass flow rate of ammonia fluid after expansion

$$\dot{m}_{9f} = [\dot{m}_7 X_7 + \dot{m}_{ar}](1 - X_9) \quad (17)$$

General mass balance of ammonia at state 9 considering control volume approaches Mass balance equation

$$\dot{m}_9 = \dot{m}_{10} \quad (18)$$

$$(\dot{m}_9 X_9 + \dot{m}_{ar9} + \dot{m}_{9I}) = \dot{m}_{10v} + \dot{m}_{10f} \quad (19)$$

Where $\dot{m}_{10} = \dot{m}_9$; $\dot{m}_9 = \dot{m}_7$

Ammonia mass balance equation

$$\dot{m}_7\xi_7 + \dot{m}_{11}\,\zeta_{11} \quad (20)$$

Where $\xi_7 = \xi_9$

Energy balance equation

$$\dot{Q}_e = \left(\dot{m}_{10v} h_{10v} + \dot{m}_{10f} h_{10f}\right) + \dot{m}_I C_{PI}(\mathrm{T}_{10} - \mathrm{T}_9) - \left(\dot{m}_{10v} h_{10v} + \dot{m}_{10f} h_{10f}\right) + \dot{m}_7 X_7 (h_9 - h_7) + \dot{m}_{ar}(h_9 - h_{11}) \quad (21)$$

3.7 Absorber and Receiver Tank

In the receiver tank, ammonia and helium gas mixture leaving the evaporator at state 10 and uncondensed ammonia gas from the condenser at state 8 get mixed with the lean solution coming from the solution heat exchanger at state 14. Ammonia vapour is readily absorbed into the lean in ammonia solution to produce rich in ammonia solution. During the absorption processes, helium gas is liberated which leaves the reservoir along with some amount of unabsorbed ammonia gas. Thus residual gas mixture (helium and unabsorbed ammonia) leaves the reservoir and moves towards flash box.

Ammonia vapour leaving the evaporator and bypass from condenser at state 10.

$$\dot{m}_{10v} = [\dot{m}_7 X_7 + \dot{m}_{ar}] X_{10} + \dot{m}_8 X_8 \quad (22)$$

Liquid ammonia leaving the evaporator

$$\dot{m}_{10f} = [\dot{m}_7 X_7 + \dot{m}_{ar}](1 - X_{10}) \quad (23)$$

Mass balance equation

$$\dot{m}_{10} + \dot{m}_{14} = \dot{m}_{12} + \dot{m}_{11} \quad (24)$$

Where $\dot{m}_{10} = \dot{m}_{10v} + \dot{m}_{10f}$

Ammonia mass balance equation

$$\dot{m}_{10}\zeta_{10} + \dot{m}_{14}\xi_{14} = \dot{m}_{12}\xi_{12} + \dot{m}_{11}\zeta_{11} \quad (25)$$

Heat rejected in the absorber is as

$$\dot{Q}_a = (\dot{m}_{12}h_{12} + \dot{m}_{11I}h_{11I} + \dot{m}_{11}h_{11}) - (\dot{m}_{10v}h_{10v} + \dot{m}_{10f}h_{10f} + \dot{m}_{10I}h_{10I} + \dot{m}_{14}h_{14}) \quad (26)$$

Heat of absorption is liberating when ammonia is absorbed in lean solution. The heat of absorption is rejecting from the absorber into the ambient.

3.8 Solution heat exchanger

In solution heat exchanger, rich solution is heat by extracting heat from the lean solution, which is return from the separator at state 13.

Mass balance for lean solution

$$\dot{m}_{13} = \dot{m}_{14} \quad (27)$$

Where, $\dot{m}_{13} = \dot{m}_3 + \dot{m}_5$

Mass balance for rich solution

$$\dot{m}_1 = \dot{m}_{12} \quad (28)$$

Ammonia mass balance

$$\xi_{13} = \xi_{14} \quad (29)$$

$$\xi_1 = \xi_{12} \quad (30)$$

Energy balance equation

$$(\dot{m}_1 h_1 + \dot{m}_{14} h_{14}) - (\dot{m}_{13} h_{13} + \dot{m}_{12} h_{12}) = 0 \quad (31)$$

Relation between mole fraction and mass fraction for ammonia is present below;

$$\xi = \frac{17.03x}{17.03x+(1-x)18.01} \quad (32)$$

The partial pressure of NH_3 in the gas mixture is defined as

$$\frac{P_{partial}}{P_{total}} = \frac{N_{NH_3}}{N_{NH_3}+N_H} \quad (33)$$

Mass flow Ratio (MFR)

The mass flow ratio (*Π*) is described as the ratio of the mass flow rate of the rich solution leaving the reservoir to the mass flow rate of pure refrigerant. It is also called as circulation ratio.

$$\Pi = \frac{\dot{m}_{12}}{\dot{m}_6} \quad (34)$$

Cycle Performance

The performance of DAR system is given by the amount of cooling by a refrigerant machine per unit heat supplied. However, coefficient of performance is also defined as refrigerant rate over the rate of heat addition at the generator.

$$COP = \frac{\dot{Q}_e}{\dot{Q}_g} \quad (35)$$

4. Result and Discussion

Present study considers the input parameters as described in Table 1 for the thermodynamic analysis of the refrigeration cycle arrangement shown in Fig. 1. Computer simulation, based on the thermodynamic modelling has been used for carrying out parametric analysis. A parametric study using EES software and it's built in property methods for aqua ammonia has been performed on the DAR cycle. Details of parametric variations are graphically presented along with the suitable tabular presentation as per the requirements for the same parametric variations.

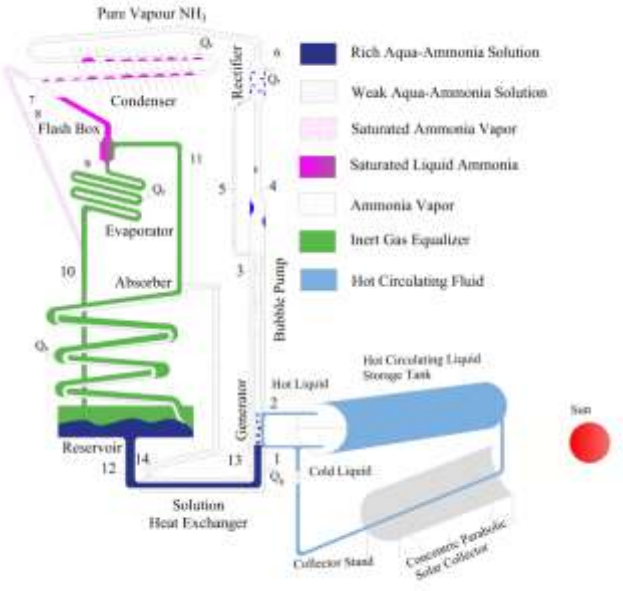

Fig. 1. Schematic diagram of diffusion absorption refrigeration cycle modelled in this study operating using solar energy.

Table 1 Input parameter and component characteristics for Diffusion Absorption refrigeration system.

Component characteristics	Value/ Range	Unit
Mass fraction of ammonia in aqua-ammonia mixture	0.28-0.73	-
Generator temperature range	140-185	°C
Acceleration due to gravity - Kanpur	9.8	m/s^2
Mass flow of strong solution	1	kg/s
System pressure	16-21	bar
Condenser temperature range	40 - 50	°C
Minimum absorber temperature	40 - 50	°C
Evaporator temperature range	(-20) to 1	°C
Generator dynamic pressure loss	0.05	bar
Bubble pump dynamic pressure loss	0.1	bar
Heat exchanger dynamic pressure loss	0.1	bar
Flash box dynamic pressure loss	0.05	bar
Pipe loss fraction	1.00%	-

Figure 2 describes clearly that coefficient of performance of DAR system is minimal up to total system pressure 1700 kPa for the given reference values as shown above the graphical presentation Fig. 2. Coefficient of performance of the system shows significant value above

pressure 1750 kPa and increases with the rise in total system pressure of the cycle. It also observes that cooling effect (Q_e) decreases slightly with rise in pressure. Hence, the increase in coefficient of performance occurs due to amount decrease in heat supplied to the generator of DAR system at varying system pressure. The graphical presentation shows a linear decrease in mass flow ratio at exit of rectifier (Π_{ref}) and bubble pump (Π_{bp}) with rise in system pressure. Because of this, the availability of the condensed liquid at evaporator inlet will drop off cooling effect. Hence, the coefficient of performance of the system will decrease with the rise in total system pressure.

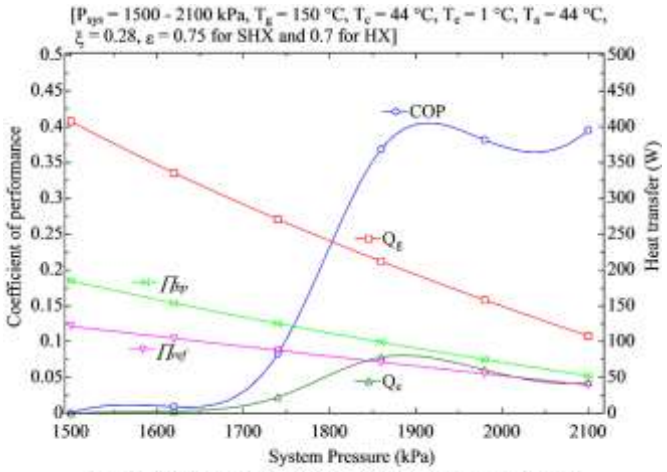

Fig. 2. Variations in coefficient of performance, mass flow ratio of refrigerant and heat transfer with total system pressure.

Table 2 Variations in coefficient of performance and other parameter with the variation in system pressure. [At P_{sys} = 1500 - 2100 kPa, T_g = 150 °C, T_c = 44 °C, T_e = 1 °C, T_a = 44 °C, ξ = 0.28, ε = 0.75 SHX, ε = 0.70 HX]

P_{sys} (kPa)	COP	Π_{bp}	Π_{ref}	Q_e (W)	Q_g (W)
1500	0.0003702	0.1854	0.1215	0.1509	407.7
1620	0.009214	0.1538	0.1045	3.092	335.6
1740	0.08331	0.1254	0.08786	22.57	270.9
1860	0.3687	0.09936	0.07145	78.23	212.2
1980	0.3816	0.07512	0.05523	60.35	158.2
2100	0.3957	0.05223	0.03915	42.7	107.9

Figure 3 delineates that coefficient of performance at generator temperature 130 °C gives highest value with the rise in ammonia mass fraction. As we know, the effectiveness of the evaporator is specific and it provides work accordingly. In generator context, the heat supplied could be increased with the increase in generator temperature. The heat supplied to the generator (Q_g) is responsible to increase the rate of refrigerant vapours. For optimum coefficient of performance, both the variables should be in right proportions. So, a metered amount of liquid refrigerant should reach at the inlet of evaporator with minimum heat removal in rectifier and condenser. This metered liquid should completely vaporize absorbing latent heat of vaporization before leaving the evaporator; producing unstinting cooling effect to get highest coefficient of performance of the system. This Fig. 3 shows that coefficient of performance decreases with increase in the generator temperature. This is owing to the increase heat supplied at higher generator temperature, which will responsible to increase the production of refrigerant vapour. This will increase the amount of liquid refrigerant at the inlet of evaporator with rejecting more heat in rectifier. The liquid refrigerant will transform into vapour form after absorbing heat as per the effectiveness of evaporator and producing cooling effect and rest liquid will pass through the evaporator without producing any cooling effect. Because of this cause, the coefficient of performance starts decreasing at high generator temperature. The range of heat supplied to a pertinent range of ammonia mass fraction provides optimum coefficient of performance is ($0.30 \le \xi \le 0.45$), (140 °C $\le T_g \le$ 160 °C).

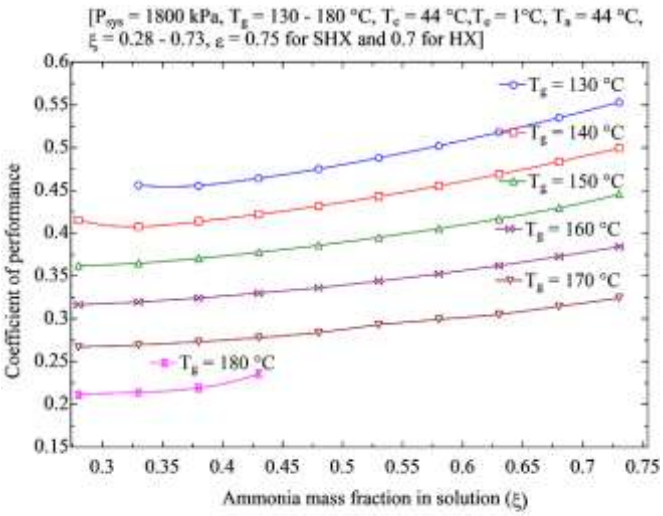

Fig. 3. Variations in coefficient of performance with the ammonia mass fraction in the solution at varying generator temperature.

Table 3 Values of coefficient of performance with the ammonia mass fraction at varying generator temperature. [At P_{sys} = 1800 kPa, T_g = 130-190 °C, T_c = 44 °C, T_e = 1 °C, T_a = 44 °C, ξ = 0.28 – 0.73, ε = 0.75 SHX, ε = 0.7 HX]

ξ	T_g=130 (°C)	T_g=140 (°C)	T_g=150 (°C)	T_g=160 (°C)	T_g=170 (°C)	T_g=180 (°C)	T_g=190 (°C)
0.28	0.0352	0.4153	0.3623	0.3166	0.2669	0.2112	0.1645
0.33	0.4562	0.4077	0.3649	0.3196	0.2694	0.214	0.5129
0.38	0.4557	0.4137	0.3706	0.3242	0.2731	0.2191	0.5247
0.43	0.4641	0.422	0.3777	0.3298	0.2777	0.2359	0.5262
0.48	0.4751	0.4317	0.3858	0.3363	0.2836	0.5228	0.5287
0.53	0.488	0.4429	0.3951	0.3439	0.2932	0.5379	0.5334
0.58	0.5022	0.4552	0.4054	0.3525	0.2991	0.5466	0.5406
0.63	0.5179	0.4688	0.4168	0.3621	0.305	0.5575	0.5507
0.68	0.5349	0.4835	0.4296	0.3727	0.3146	0.5713	0.5639
0.73	0.5531	0.4994	0.4456	0.3843	0.3242	0.5888	0.5805

Figure 4 shows variation in coefficient of performance and heat rejection to the cooling media of rectifier, condenser and absorber with the generator temperature. The graphical presentation shows, coefficient of performance decreases with the increase in the heat rejection by the components of DAR cycle. The major impacts on coefficient of performance by the heat removal in rectification process to put away any possibility of liquid drops in the vapour of refrigerant. It is clearly shown form the Fig. 4 that the gradient of heat transfer by the condenser (Q_c) and the absorber (Q_a) is almost similar and increase gradually with the increase in generator temperature. While, the heat removal in rectifier (Q_r) increases drastically. This is owing to the excess heat supplied to the aqua ammonia solution in the generator could not take part and rejected through the rectifier as shown by the trends of curve above generator temperature 160 °C. Hence, shows decrease in coefficient of performance of DAR cycle.

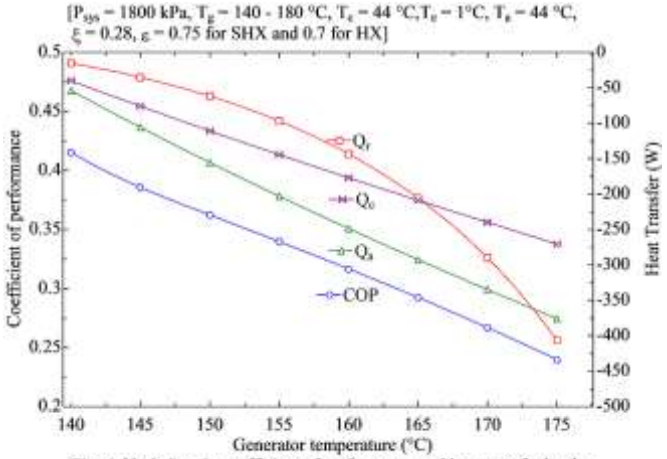

Fig. 4. Variations in coefficient of performance and heat transfer by the components in DAR system at varying generator temperature.

Table 4 Values of coefficient of performance and heat transfer by the components at varying generator temperature. [At P_{sys} = 1800 kPa, T_g = 140 - 185 °C, T_c = 44 °C, T_e = 1 °C, T_a = 44 °C, ξ = 0.28, ε = 0.75 SHX, ε = 0.7 HX]

T_g (°C)	COP	Q_r (W)	Q_c (W)	Q_a (W)
140	0.4153	-15.45	-40	-53.9
145	0.3857	-35.27	-76.06	-105.9
150	0.3623	-61.75	-110.8	-105.9
155	0.3397	-96.89	-144.5	-203.1
160	0.3166	-205.8	-208.8	-292.6
165	0.2924	-143.5	-177.1	-248.7
170	0.2669	-290	-239.9	-334.9
175	0.2398	-406.4	-270.6	-376
180	0.2112	-572.7	301.8	-416.7
185	0.1817	-820.8	-336.3	-460.4

Figure 5 delineates the relation between coefficient of performance and lean ammonia concentration with variations of ammonia mass fraction in aqua ammonia solution. It shows for varying ammonia mass fraction, coefficient of performance increases linearly and gives highest value at the generator temperature 140 °C, while no marginal decrease shown in the lean concentration for same temperature. Similar pattern of coefficient of performance shown for the generator temperature 150 °C and 160 °C but value of coefficient of performance is lower for 160 °C. The patterns for lean ammonia concentration does not show same effect as previous, but shows drastic decrease in curve for ammonia mass fraction more than 0.60.

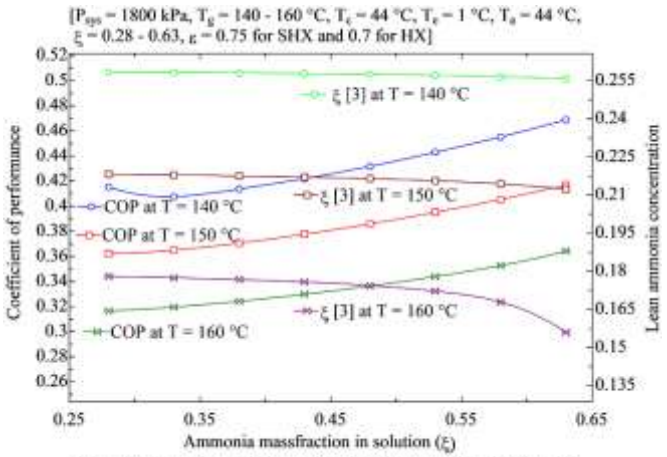

Fig. 5. Variations in coefficient of performance and lean concentration of ammonia with mass fraction of ammonia in aqua ammonia solution.

Figure 6 shows variations in mass flow rate of auxiliary gas with ammonia mass fraction in aqua ammonia solution at varying generator temperature. In the diffusion absorption cycle, mass flow rate of auxiliary gas is responsible to lower the partial pressure of condensed refrigerant liquid in the evaporator and helps to produce cooling effect with the evaporation of refrigerant liquid at lower temperature. Since, the cooling capacity is responsible to increase the coefficient of performance of the DAR cycle, so the coefficient of performance increases with increase in cooling capacity. As the generator temperature increases with the ammonia mass fraction, mass flow rate of inert gas also increases linearly to lower the partial pressure of liquid refrigerant and hence, increasing cooling effects. Consequently, coefficient of performance of the DAR system will increase.

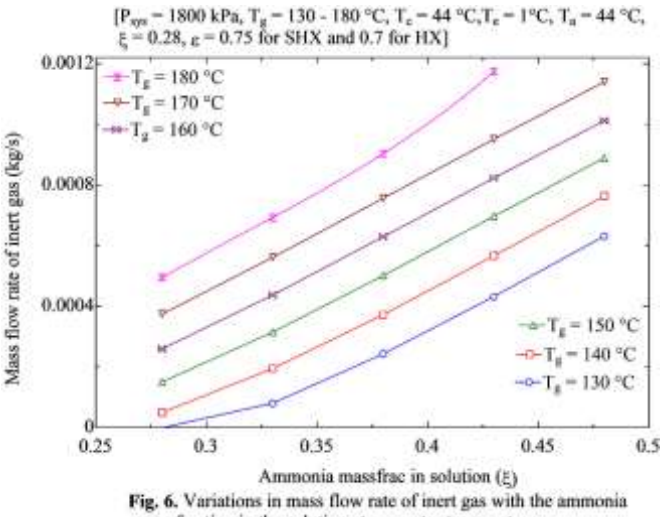

Fig. 6. Variations in mass flow rate of inert gas with the ammonia mass fraction in the solution at generator temperature.

Table 5 Values of mass flow rate of inert gas (kg/s) with the ammonia mass fraction at varying generator temperature. [At P_{sys}= 1800 kPa, T_g = 140 - 185 °C, T_c = 44 °C, T_e = 1 °C, T_a = 44 °C, ξ = 0.28 - 0.73, ε = 0.75 SHX, ε = 0.7 HX]

ξ	T_g=130 (°C)	T_g=140 (°C)	T_g=150 (°C)	T_g=160 (°C)	T_g=170 (°C)	T_g=180 (°C)	T_g=190 (°C)
0.28	0.00000127	0.0000488	0.0001501	0.0002594	0.000374	0.0004948	0.0007147
0.33	0.0000796	0.0001944	0.0003144	0.0004369	0.000561	0.0006929	0.002861
0.38	0.0002426	0.0003723	0.0005014	0.000629	0.0007566	0.0009036	0.002877
0.43	0.0004322	0.0005668	0.000697	0.0008238	0.0009514	0.001174	0.002891
0.48	0.000632	0.0007641	0.0008901	0.001012	0.001141	0.002904	0.002894
0.53	0.0008295	0.0009543	0.001073	0.0011868	0.001332	0.002885	0.002884
0.58	0.001019	0.001134	0.001243	0.0013438	0.001547	0.002861	0.002862
0.63	0.001197	0.0013	0.0014	0.0014809	0.0018286	0.002825	0.002826
0.68	0.001363	0.001455	0.001546	0.0015982	0.0022424	0.002776	0.002643
0.73	0.00152	0.0016	0.001695	0.0016979	0.002879	0.002714	0.002096

Figure 7 shows miscellaneous graphical representation for different independent parameters. It depicts the variation of coefficient of performance and heat transfers with the generator temperature. It is obvious facts that rise in the generator temperature depend upon solar energy supplied to the generator. It shows heat supplied to the generator (Q_g) increases parabolically with the increase in the generator temperature. This increase in energy will energize the rate of evaporation of ammonia and water, successively increase in irreversibilities and hence falls down in coefficient of performance despite increase in cooling effect of DAR cycle. It also shows the profile in graph for Π_{bp}, Π_{ref} at increasing generator temperature. It shows at increasing generator temperature, mass flow ratio of refrigerant is unaffected and shows linear pattern but the mass flow ratio of bubble pump increases parabolically above the generator temperature 155°C. Since graphs shows slight increase in cooling effect compared to more heat supplied, hence the coefficient of performance decreases at increasing generator temperature.

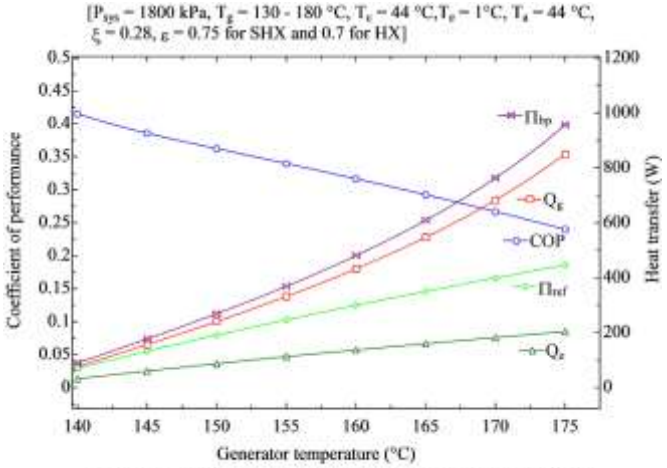

Fig. 7. Variations in coefficient of performance and heat transfer with the generator temperature.

Figure 8 illustrates that mass flow rate at the exit of bubble pump and at the inlet of condenser increases with the rise in ammonia mass fraction in the rich solution. Due to this, refrigerant vapour at the inlet of condenser will increase, which results more condensed liquid refrigerant available at the inlet of the evaporator for producing more cooling capacity without any more heat input to the DAR cycle. Since cooling effect increases without any extra heat input. Consequently, coefficient of performance will increase.

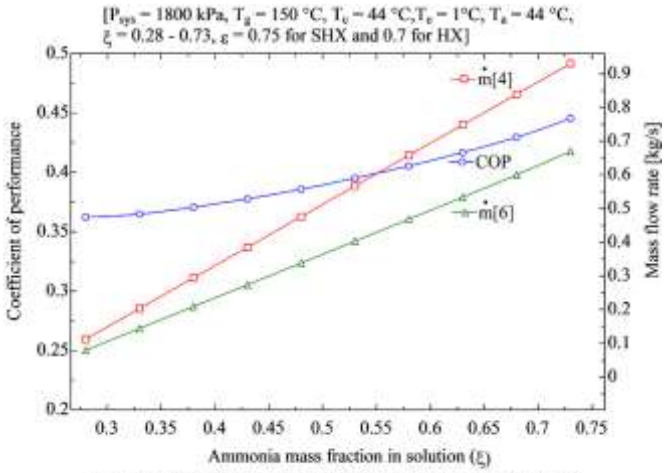

Fig. 8. Variations in coefficient of performance and mass flow rate with the ammonia mass fraction in the solution.

Table 7 Values of coefficient of performance and mass flow rate at exit of bubble pump and rectifier for refrigerant at variable ammonia mass fraction in solution. [At P_{sys} = 1800 kPa, Tg = 150 °C, Tc = 44 °C, Te = 1 °C, Ta = 44 °C, ξ = 0.28 – 0.73, ε = 0.75 SHX, ε = 0.7 HX]

ξ	COP	$\dot{m}_4$[kg/s]	$\dot{m}_6$[kg/s]
0.28	0.3623	0.1121	0.07963
0.33	0.3649	0.2031	0.1443
0.38	0.3706	0.2941	0.209
0.43	0.3777	0.3851	0.2737
0.48	0.3858	0.476	0.3385
0.53	0.3951	0.567	0.4034
0.58	0.4054	0.6579	0.4684
0.63	0.4168	0.7488	0.5337
0.68	0.4296	0.8397	0.5998
0.73	0.4456	0.9306	0.67

Figure 9 illustrates slight linear increase in coefficient of performance with the increase in evaporator temperature at the exit of evaporator keeping constant ammonia concentration in the aqua ammonia solution at varying generator temperature. The graph also shows that the highest value of coefficient of performance is at 140 °C generator temperature and in the case of temperature rise; subtraction begins. The highest value of coefficient of performance found at 274 K evaporator temperature for the given set of reference values as given in the Table 5 and in the Fig. 9. This graphical presentation shows that the DAR cycle is more useful in cooling purposes as compared to freezing.

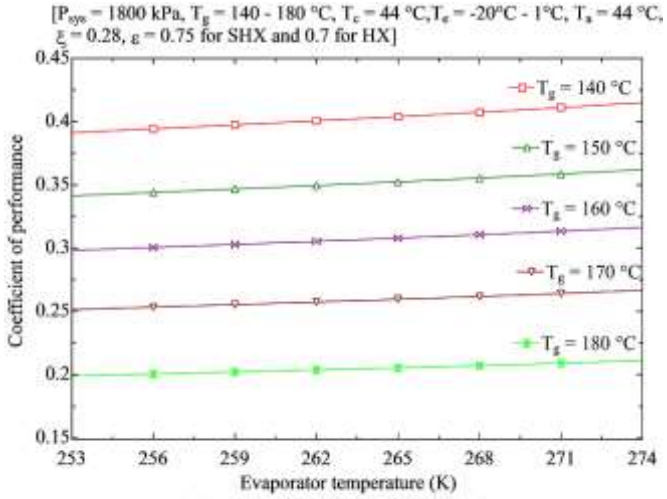

Fig. 9. Variations in coefficient of performance with the evaporator temperature at varying generator temperature.

Table 8 Values of coefficient of performance with the evaporator temperature at varying generator temperature. [At P_{sys} = 1800 kPa, T_g = 140-185 °C, T_c = 44 °C, T_e = -20 °C to 1 °C, T_a = 44 °C, ξ = 0.28, ε = 0.75 SHX, ε = 0.7 HX]

T_e (K)	T_g=140 (°C)	T_g=150 (°C)	T_g=160 (°C)	T_g=170 (°C)	T_g=180 (°C)
253	0.3913	0.3414	0.2983	0.2514	0.1989
256	0.3944	0.344	0.3006	0.2534	0.2005
259	0.3975	0.3467	0.303	0.2554	0.2021
262	0.4007	0.3495	0.3054	0.2574	0.2037
265	0.404	0.3524	0.3079	0.2595	0.2054
268	0.4074	0.3554	0.3105	0.2618	0.2071
271	0.4111	0.3586	0.3134	0.2641	0.209
274	0.4151	0.3621	0.3164	0.2667	0.2111

Figure 10 shows variations in coefficient of performance with pressure loss and without pressure losses at varying generator temperature. It is graphically shows that the pressure losses affect the coefficient of performance at lower generator temperature (i.e. 140 °C) for the given set of reference values. It shows that at the generator temperature 140 °C, the gain in coefficient of performance is about 5% and at the generator temperature 160 °C, there is 2.75 % gain, when neglecting pressure losses. This gain percentage in coefficient of performance reduces at higher temperature. The difference in coefficient of performance could be neglected when generator temperature more than 180 °C. Therefore, at higher generator temperature, the effect of piping and dynamic pressure losses can be neglected.

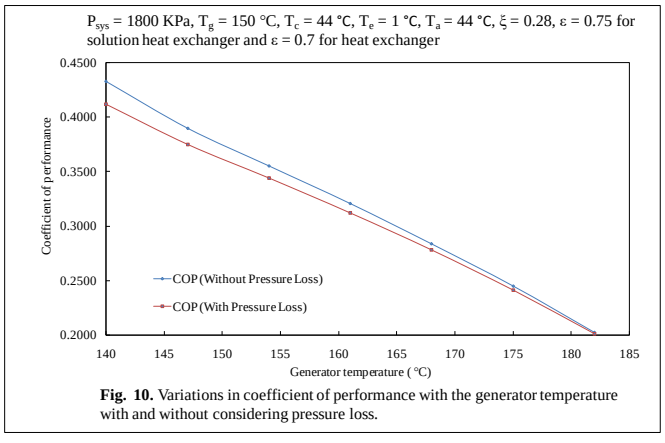

Fig. 10. Variations in coefficient of performance with the generator temperature with and without considering pressure loss.

Table 9 Values of coefficient of performance with the generator temperature with considering the pressure losses in the DAR cycle. [At P_{sys} = 1800 kPa, T_g = 140-185 °C, T_c = 44 °C, T_e = 1 °C, T_a = 44 °C, ξ = 0.28, ε = 0.75 SHX, ε = 0.7 HX]

T_g (°C)	COP (With Pressure Loss)	COP (Without Pressure Loss)	P_{sys} (kPa)
140	0.3916	0.4122	1800
147	0.3600	0.375	1800
154	0.3327	0.3439	1800
161	0.3034	0.312	1800
168	0.2723	0.2779	1800
175	0.2367	0.2409	1800
182	0.2003	0.2013	1800

Results obtained in our study are compared with previous experimental and numerical studies data [3], [5] and [11] to validate the model. Since these three have different operating conditions. So, for comparison, it is necessary that the operating conditions should be almost similar to the compared experimental or numerical data. Therefore, the comparison is made separately for each study under the specific operating conditions and presented in Table 10. The comparison Table shows that the obtained values of our model almost near or coincide with the data presented in each study.

Table 10 Comparison between our obtained results and previous published data.

	Zohar et al. Numerical [3]	Our Obtained Result	Srikhirin et al. experiment [5]	Our Obtained Result	Chen et al. experiment [11]	Our Obtained Result
COP	0.20 - 0.21	0.207	0.09 - 0.16	0.157	0.1 - 0.20	0.164

The parametric values obtained for different reference state or node points respectively as given in Fig. 1 are presenting in the Tables 11-14 for given reference values. The Table 12 and 14 presents the data for 3 °C sub-cooling while Table 11 and 13 for saturated liquid, at the exit of the condenser, without and with considering pressure loss respectively. The data presented in Table 11-14 shows 1.3% gain in refrigerating effect when 3 °C sub-cooling gets at the condenser exit. The coefficient of performance increased up to 23% for ammonia mass fraction ranges 0.28 to 0.58% and a 3.02% loss in performance noticed when a 10°C increase in evaporator temperature.

Table 11 Values of pressure, temperature, concentration, flow rate and enthalpy with the state point of the cycle without pressure losses. [At P_{sys}= 1800 kPa, T_g = 150 °C, T_c = 44 °C, T_e = 1 °C, T_a = 44 °C, ξ = 0.28, ε = 0.75 for SHX and ε = 0.7 for HX].

State point	Pressure P (bar)	Temperature T (°C)	Concentration ξ(kg/kg of mixture)	Enthalpy h (kJ/kg)	Flow rate ṁ (kg/s)	Pressure P Inert gas (bar)	Temperature of inert gas T (°C)	Concentration of refrigerants	Enthalpy of inert gas h (kJ/kg)	Flow rate of inert gas ṁ (kg/s)	Quality of refrigerant
1	18	135.4	0.28	417.7	1						0
2	17.79	150	0.28	656.8	1						0.1121
3	17.98	150	0.7699	1833	0.1121						1
4	18	150	0.2181	509.9	0.8879						-0.001
5	17.98	150	0.995	1599	0.07963						1.001
6	17.98	150	0.2181	509.9	0.03249						0.0007163
7	17.98	44	0.995	207.3	0.07963						-0.001
8	By	Pass	Node			By	Pass	Node			
9	0.67	-41.14	0.995	207.3	0.07963	1693	90.49	100	1764	0.0001501	0.2838
10	0.6382	1	0.995	1304	0.07963	1684	1	100	1299	0.0001501	0.9979
11						1710	90.48	100	1764	0.0001501	
12	18.1	90.48	0.28	211.8	1						-0.001
13	17.83	150.1	0.2181	510.1	0.9204						-0.001
14	17.5	100.8	0.2181	286.4	0.9204						-0.001

Table 12 Values of pressure, temperature, concentration, flow rate and enthalpy with the state point of the cycle without pressure losses. [At P_{sys}= 1800 kPa, T_g = 150 °C, T_c = 44 °C, T_e = 1 °C, T_a = 44 °C, ξ = 0.28, ε = 0.75 for SHX and ε = 0.7 for HX].

State point	Pressure P (bar)	Temperature T (°C)	Concentration ξ(kg/kg of mixture)	Enthalpy h (kJ/kg)	Flow rate ṁ (kg/s)	Pressure P Inert gas (bar)	Temperature of inert gas T (°C)	Concentration of refrigerants	Enthalpy of inert gas h (kJ/kg)	Flow rate of inert gas ṁ (kg/s)	Quality of refrigerant
1	18	135.4	0.28	417.7	1						0
2	17.79	150	0.28	656.8	1						0.1121
3	17.98	150	0.7699	1833	0.1121						1
4	18	150	0.2181	509.9	0.8879						-0.001
5	17.98	150	0.995	1599	0.07963						1.001
6	17.98	150	0.2181	509.9	0.03249						0.0007163
7	17.98	41	0.995	192.3	0.07963						-0.001
8	By	Pass	Node			By	Pass	Node			
9	0.67	-41.14	0.995	192.3	0.07963	1693	90.49	100	1764	0.0001473	0.2731
10	0.638	1	0.995	1304	0.07963	1684	1	100	1299	0.0001473	0.9979
11						1710	90.48	100	1764	0.0001473	
12	18.1	90.48	0.28	211.8	1						-0.001
13	17.83	150.1	0.2181	510.1	0.9204						-0.001
14	17.5	100.8	0.2181	286.4	0.9204						-0.001

Table 13 Values of pressure, temperature, concentration, flow rate and enthalpy with the state point of the cycle with pressure losses. [At P_{sys}= 1800 kPa, T_g = 150 °C, T_c = 44 °C, T_e = 1 °C, T_a = 44 °C, ξ = 0.28, ε = 0.75 for SHX and ε = 0.7 for HX].

State point	Pressure P (bar)	Temperature T (°C)	Concentration ξ(kg/kg of mixture)	Enthalpy h (kJ/kg)	Flow rate ṁ (kg/s)	Pressure P Inert gas (bar)	Temperature of inert gas T (°C)	Concentration of refrigerants	Enthalpy of inert gas h (kJ/kg)	Flow rate of inert gas ṁ (kg/s)	Quality of refrigerant
1	18	135.4	0.28	417.7	1						0
2	17.74	150	0.28	658.6	1						0.111
3	17.88	150	0.7714	1835	0.111						1
4	17.8	150.1	0.2186	510.1	0.889						-0.001
5	17.7	150	0.995	1599	0.07906						1.001
6	17.7	150.1	0.2186	511.2	0.03198						-0.001
7	17.6	44	0.995	207.3	0.07906						-0.001
8	By	Pass	Node			By	Pass	Node			
9	0.72	-39.8	0.995	207.3	0.07906	1726	90.47	100	1764	0.0001516	0.2803
10	0.6919	1	0.995	1302	0.07906	1726	1	100	1299	0.0001516	0.9971
11						1726	90.47	100	1764	0.0001516	
12	17.82	90.47	0.28	211.8	1						-0.001
13	18.13	150.1	0.2186	509.9	0.9209						-0.001
14	18.08	100.8	0.2186	286.3	0.9209						-0.001

Table 14 Values of pressure, temperature, concentration, flow rate and enthalpy with the state point of the cycle with pressure losses. [At P_{sys}= 1800 kPa, T_g = 150 °C, T_c = 44 °C, T_e = 1 °C, T_a = 44 °C, ξ = 0.28, ε = 0.75 for SHX and ε = 0.7 for HX].

State point	Pressure P (bar)	Temperature T (°C)	Concentration ξ(kg/kg of mixture)	Enthalpy h (kJ/kg)	Flow rate ṁ (kg/s)	Pressure P Inert gas (bar)	Temperature of inert gas T (°C)	Concentration of refrigerants	Enthalpy of inert gas h (kJ/kg)	Flow rate of inert gas ṁ (kg/s)	Quality of refrigerant
1	18	135.4	0.28	417.7	1						0
2	17.74	150	0.28	658.6	1						0.111
3	17.88	150	0.7714	1835	0.111						1
4	17.8	150.1	0.2186	510.1	0.889						-0.001
5	17.7	150	0.995	1599	0.07906						1.001
6	17.7	150.1	0.2186	511.2	0.03198						-0.001
7	17.6	41	0.995	192.3	0.07906						-0.001
8	By	Pass	Node			By	Pass	Node			
9	0.72	-39.81	0.995	192.3	0.07906	1726	90.47	100	1764	0.0001488	0.2696
10	0.6917	1	0.995	1302	0.07906	1726	1	100	1299	0.0001488	0.9971
11						1726	90.47	100	1764	0.0001488	
12	17.82	90.47	0.28	211.8	1						-0.001
13	18.13	150.1	0.2186	509.9	0.9209						-0.001
14	18.08	100.8	0.2186	286.3	0.9209						-0.001

5. Conclusion

A computer simulation basis thermodynamic modelling has been carried out in the present work to forebode the performance of the DAR cycle for various generator, evaporator and condenser temperatures including concentrations of the refrigerant in ammonia-water solution. It concludes that in general, the performance of DAR cycle is poor owing to big amount of heat lost during cooling process in rectifier and absorber. The gain in coefficient of performance is 2.29% when the mass fraction of ammonia increases by 35.7% from its initial value 0.28. When the mass fraction of ammonia is increase by 89.29%, the gain percentage in coefficient of performance founds 9.05. The total system pressure should be more than or equal to condensing pressure of the refrigerant. The coefficient of performance is higher if the system pressure more than condenser temperature. The study shows that at the generator temperature 140 °C, the gain in coefficient of performance is about 5% and at the generator temperature 160 °C, there is 2.75 % gain, when neglecting pressure losses. This gain percentage in coefficient of performance reduces at higher temperature. The difference in coefficient of performance could be neglected when generator temperature more than 180 °C. Therefore, at higher generator temperature, the effect of piping and dynamic pressure losses can be neglect.

The aqua ammonia DAR cycle can be used for maintaining temperatures below 0 °C but in such situation coefficient of performance will be poor. The ammonia water mixture is not being a good impending pair for absorption refrigeration cycles, operating with lower generator temperatures. The performance of aqua ammonia DAR cycle can increase by changing heat transfer medium as water-cooling in place of air-cooling for condenser, rectifier and absorber like such countries where the ambient temperature is too high in summer season as in India. The additional advantage of this system is that the system can utilize heat sources like solar, geothermal and industrial waste or others in place of conventional energy sources.

6. References

Electronic Resource

[1] Von Platen BC, Munters CG, US Patent 1, 685-764; 1928.

[2] www.dometic.com (formerly known as Electrolux in Europe) 2004.

Journal paper

[3] Zohar A, Jelinek M et al. (2005), "Numerical Investigation of a Diffusion Absorption Refrigeration Cycle", International Journal of Refrigeration, Vol. 28, pp. 515-525.

[4] Giuseppe Starace, Lorenzo De Pascalis (2011), "An Advanced Analytical Model of the Diffusion Absorption Refrigerator Cycle", International Journal of Refrigeration, Vol. 35, pp. 605-612.

[5] P. Srikhirin, S. Aphornratana, "Investigation of a diffusion absorption refrigerator," Applied Thermal Engineering, Vol. 22, pp. 1181-1193.

[6] Wang Q et al. (2011), "A Numerical Investigation of a Diffusion Absorption Refrigerator Operating with the Binary Refrigerant for Low Temperature Applications", Applied Thermal Engineering, Vol. 31, pp.1763-1769.

[7] Adnan Sozen, Tayfun Menlik, Engin Ozbas "The effect of ejector on the performance of DAR system: An experimental study" Applied Thermal Engineering 33-34 (2012) pp 44-53.

[8] N. Ben Ezzine, R. Garma, A. Bellagi "A numerical investigation of a diffusion absorption refrigeration cycle based on R124-DMAC mixture for solar cooling" Energy 35 (2010) pp 1874–1883.

[9] N. Ben Ezzine, R. Garma, M. Bourouis, A. Bellagi "Experimental studies on bubble pump operated diffusion absorption machine based on light hydrocarbons for solar cooling" Renewable Energy 35 (2010) pp 464–470.

[10] Handong Wanga "A new style solar driven diffusion absorption refrigerator and its operating

characteristics" Energy Procedia 18 (2012) pp 681-692.

[11] Chen J, Kin K J, Herold K E (1996), Performance Enhancement of a Diffusion Absorption *Refrigeration*, Vol. 19, No. 3, pp. 208-218.

[12] Acuna A. Velázquez N, Sauceda D, Rosales P, Suastegui A, Ortiz A "Influence of a compound parabolic concentrator in the performance of a solar diffusion absorption cooling system" Applied Thermal Engineering, volume 102. 5 June 2016, pp. 1374 -1383.

[13] Koyfman A et al. (2003), "An Experimental Investigation of Bubble Pump Performance for Diffusion Absorption Refrigeration System with Organic Working Fluids", Applied Thermal Engineering, Vol. 23, pp.1881-1894.

[14] Zohar A, Jelinek M et al. (2008), "The Influence of the generator and bubble pump configuration on the performance of diffusion absorption refrigeration system", International Journal of Refrigeration, Vol. 31, pp. 962-969.

[15] Ahmed Q. K. (2018) "Assessment of the performance for a new design of storage solar collector" International Journal of Renewable Energy and Review, Vol.8, No.1, March, 2018, pp. 250-257.

7. Nomenclature

Symbol	Description of Symbol	Symbol	Description of Symbol
$\mathring{Q}$	Heat transfer rate (J/s) or (W)	SHX	Solution heat exchanger
T	Temperature (°C, K)	HX	Heat exchanger
h	Enthalpy (kJ/Kg)	N	Number of Moles for specific constituents
P	Pressure (kPa, bar)	**Subscripts**	
ξ	Mass fraction of ammonia in liquid phase	v and *f*	Stands for vapour or gas and liquid
x	Mole fraction of ammonia in liquid phase	g	Generator
ζ	Mass fraction of ammonia in vapour phase	r	Rectifier
y	Mole fraction of ammonia in vapour phase	a	Absorber
DAR	Diffusion absorption refrigeration	c	Condenser
COP	Coefficient of performance	e	Evaporator
$\mathring{m}$	Mass flow rate (kg/s)	ar	Ammonia gas residuals
X	Quality of vapour	rh	Recuperative heat exchanger
Π	Mass flow ratio	sys	Total system pressure
I	Inert Helium gas	Numeric	1,2,3,...System's point designation
ε	Effectiveness of heat exchanger		